REVIEW

Membrane microheterogeneity: Förster resonance energy transfer characterization of lateral membrane domains

**Luís M. S. Loura · Fábio Fernandes ·
Manuel Prieto**

Abstract Lateral membrane heterogeneity, in the form of lipid rafts and microdomains, is currently implicated in cell processes including signal transduction, endocytosis, and cholesterol trafficking. Various biophysical techniques have been used to detect and characterize lateral membrane domains. Among these, Förster resonance energy transfer (FRET) has the crucial advantage of being sensitive to domain sizes smaller than 50-100 nm, below the resolution of optical microscopy but, apparently, similar to those of rafts in cell membranes. In the last decade, several formalisms for the analysis of FRET in heterogeneous membrane systems have been derived and applied to the study of microdomains. They are critically described and illustrated here.

Keywords FRET · Lipid bilayer · Lipid raft · Membrane phase separation · Phase diagram

The more you see: spectroscopy in molecular biophysics.

L. M. S. Loura (✉)
Faculdade de Farmácia, Universidade de Coimbra,
Pólo das Ciências da Saúde, Azinhaga de Santa Comba,
3000-548 Coimbra, Portugal
e-mail: lloura@ff.uc.pt

L. M. S. Loura
Centro de Química de Évora, Rua Romão Ramalho, 59,
7000-671 Évora, Portugal

F. Fernandes
Department of Membrane Biophysics,
Max-Planck Institute for Biophysical Chemistry,
Am Fassberg 11, 37077 Göttingen, Germany

M. Prieto
Centro de Química Física Molecular and Institute
of Nanosciences and Nanotechnologies, Complexo I,
Instituto Superior Técnico, Av. Rovisco Pais,
1049-001 Lisbon, Portugal

Abbreviations

BSM	Brain sphingomyelin
CFM	Confocal fluorescence microscopy
Chol	Cholesterol
Dansyl-PC	2-[12-[(5-Dimethylamino-1-naphthalenesulfonyl)amino]dodecanoyl]-PC
DHE	Dehydroergosterol
DiIC$_{12}$(3)	1,1′-Didodecyl-3,3,3′,3′-tetramethylindocarbocyanine
DiIC$_{18}$(3)	1,1′-Dioctadecyl-3,3,3′,3′-tetramethylindocarbocyanine
DMPC	1,2-Dimyristoyl-*sn*-glycero-3-phosphocholine
DOPC	1,2-Dioleoyl-*sn*-glycero-3-phosphocholine
DPH	1,6-Diphenylhexatriene
DPH-PC	1-Palmitoyl-2-[3-(diphenylhexatrienyl)propanoyl]-*sn*-glycero-3-phosphocholine
DPPC	1,2-Dipalmitoyl-*sn*-glycero-3-phosphocholine
DPPS	1,2-Dipalmitoyl-*sn*-glycero-3-phosphoserine
DSPC	1,2-Distearoyl-*sn*-glycero-3-phosphocholine
FRET	Förster resonance energy transfer
ld	Liquid disordered
lo	Liquid ordered
Marina Blue	1-[[(6,8-Difluoro-7-hydroxy-4-methyl-2-oxo-2*H*-1-benzopyran-3-yl)acetyl]oxy]
NBD	7-Nitrobenz-2-oxa-1,3-diazol-4-yl
NBD-DLPE	*N*-NBD-1,2-dilauroyl-*sn*-glycero-3-phosphoethanolamine
NBD-DMPE	*N*-NBD-dimyristoylphosphatidylethanolamine

NBD-DPPE	N-NBD-1,2-dihexadecanoyl-sn-glycero-3-phosphoethanolamine
NBD-PC	1-Palmitoyl-2-[12-NBD-aminododecanoyl]-sn-glycero-3-phosphocholine
PC	Phosphatidylcholine
PI(4,5)P$_2$	Phosphatidylinositol-4,5-bisphosphate
PIP$_2$	Phosphatidylinositol bisphosphate
POPC	1-Palmitoyl-2-oleoyl-sn-glycero-3-phosphocholine
POPE	1-Palmitoyl-2-oleoyl-sn-glycero-3-phosphoethanolamine
PS	Phosphatidylserine
PSM	Palmitoyl-SM
RDF	Radial distribution function
Rh-DMPE	N-(lissamine–rhodamine B)-dimyristoyl-phosphatidylethanolamine
Rh-DOPE	N-(lissamine–rhodamine B)-dioleoylphosphatidylethanolamine
Rh-DPPE	N-(lissamine–rhodamine B)-dipalmitoylphosphoethanolamine
SM	Sphingomyelin
t-PnA	trans-Parinaric acid

Membrane domains, model systems, phase diagrams and energy transfer

The fluid mosaic membrane model, which assumed homogeneous distribution of lipids where the proteins were adsorbed/inserted, was accepted for a long time in biochemistry (Singer and Nicholson 1972), because within this simple framework a significant number of observations were rationalized. However, lateral phase separation in lipid systems, in the form of so-called membrane domains, has long been recognized experimentally (Shimshick and McConnel 1973) and, later, theoretically, for example as described in two recent works (Putzel and Schick 2008; Niemelä et al. 2009). The existence of domains is a direct consequence of the non-ideality of lipid mixtures, and thus happens in the absence of proteins, although the latter can modulate membrane domains, as recognized for a long time (Morrow et al. 1986). Therefore, a more realistic concept for the membrane is currently available (Mouritsen 2005), and in a cell the effect of the cytoskeleton cannot be ignored (Goswami et al. 2008).

Regarding model systems of membranes, it is common to discuss their limitations. Whereas binary lipid mixtures are still widely used, the most complex accessible systems are ternary mixtures (eventually with the addition of a small amount of a fourth component; Silva et al. 2007; Pokorny et al. 2006). This is because of the practical limitation of describing a phase diagram beyond the Gibbs triangle, and certainly it is very far away from cell membranes, in which hundreds of natural lipids have been classified. Additionally, in most studies of model systems a situation of thermodynamic equilibrium is assumed (although this can be a very slow process even for a situation of strong lipid mismatch; de Almeida et al. 2002), at variance with a living cell which is never under equilibrium. However, model systems rationalized in the framework of phase diagrams have two advantages.

1 They enable simple characterization and description of the system. Immediate information is obtained from direct visual inspection, i.e., the types of co-existing phases for a specified lipid composition. By far, one of the more important contributions of these types of studies is the concept of cholesterol (Chol)-enriched liquid ordered (lo) and Chol-poor liquid disordered (ld) phases (Ipsen et al. 1987).

2 They enable a quantitative approach to the system, from which it is possible to predict behaviour. This would not be feasible in a model system closer to reality.

This paper reviews the formalisms currently used for detection and characterization of lipid domains in model membranes using Förster resonance energy transfer (FRET) spectroscopy. Although qualitative application of FRET methodology can be carried out, if a quantitative approach to the study of membrane domains is intended, and this means determination of their size, in addition to knowledge of the lipid phase diagram the thermodynamic tie-lines should also be known. It should be stressed that their determination can be quite complex in ternary systems (de Almeida et al. 2003). From the tie-lines and the lever rule, the amount of each phase and their composition are derived. On thermodynamic grounds, phase separation would go to completion, but often this does not happen, i.e., small size domains exist, because of a decrease of line tension and a compensating entropic contribution, among other factors (Simons and Vaz 2004). Therefore, from the diagram, we can anticipate the existence of domains, but no information about their size, shape, and dynamics is available. Microscopy techniques are invaluable on this regard, but they are limited by the lateral resolution of the microscope ($\sim$300 nm), a technical limitation that, however, has been reduced significantly in recent years (Hell 2009). This can hamper its application to lipid domains, because there is broad and consistent evidence that the domains in natural membranes are in the nanoscopic size range (Jacobson et al. 2007), as frequently occurs in binary model systems, where, e.g., the lo/ld phase co-existence could not be detected by microscopy (Veatch and Keller 2005).

Förster resonance energy transfer is a dipole–dipole interaction in which energy goes from one molecule (donor) to another suitable molecule (acceptor). The rate constant has explicit distance dependence, and the transfer is operative in the 1–10 nm range. In most applications of FRET to biological systems only one pair of molecules interacts, a situation in which the transfer kinetics is very simple, enabling easy determination of distances at the molecular scale (the so-called Stryer's "molecular ruler" designation; Stryer and Haugland 1967). At variance, in membranes, for each donor there is an ensemble of acceptors at different distances, and, as described below, the kinetics becomes much more complex. If suitable formalisms are applied, and time-resolved data are used, it is possible to obtain topological information about the system, i.e., to assess the presence of membrane domains and to estimate their size. If a quantitative model is to be applied, in addition to knowledge of the lipid phase diagram, a detailed photo-physical characterization of the probes to be used (donor and acceptor), namely their preference for a specific membrane phase (partition coefficient determination) should also be conducted. It is noteworthy that the range of distances where FRET happens is also on the nano-scale, so FRET is very suited to determination of the small domains, which otherwise are not perceived. Other biophysical methodologies used for their detection are described in a recent review (Goñi et al. 2008). It should be stressed that no dynamic information about the system is obtained from this type of FRET study, and only a frozen snapshot of the system topology (lipid lateral separation) is obtained. To assess dynamics, other approaches such as fluorescence correlation spectroscopy (Ries et al. 2009), or single particle tracking (Sergé et al. 2008), should be used.

One specific type of membrane domain is the so-called raft, initially operationally defined as the insoluble fraction obtained in detergent extraction methodology applied to membranes, and later associated to the lo phases with a specific lipid composition (Jacobson et al. 2007). Because of rafts' relevance in a variety of cell processes including signal transduction, endocytosis, and cholesterol traffick-ing, this concept was very important in the way that it bridged membrane biophysics and cell biology. Regarding FRET, it should also be mentioned that quantitative work has also been carried out at the cellular level (e.g., Sharma et al. 2004), in addition to an impressive number of applications, namely of the GFP family, in which FRET was used to determine co-localization at the molecular scale (Takanishi et al. 2006). These works are not reviewed here, as our focus lies in the formalisms and applications of FRET spectroscopy (rather than microscopy) to membrane model systems.

Qualitative approaches

In FRET studies, the most commonly used experimental observable is the so-called FRET efficiency, E. In most cases, it is calculated from the ratio of intensity of donor steady-state emission in the presence (I_{DA}) and absence (I_D) of the FRET acceptor:

$$E = I_{DA}/I_D \tag{1}$$

Alternatively, E may be calculated from the ratio of the integrals of the time-resolved donor emission in the presence ($i_{DA}(t)$) and absence ($i_D(t)$) of the acceptor:

$$E = 1 - \int_0^\infty i_{DA}(t)\, dt \left/ \int_0^\infty i_D(t)\, dt \right. \tag{2}$$

This latter equation also enables theoretical computation of E, after numerical integration of the donor decay law in the presence of the acceptor (see the following sections).

Förster resonance energy transfer-based approaches to the problem of recognizing the formation of lateral domains in a lipid bilayer always depend on the use of either a FRET donor or acceptor molecule (or preferentially both) with higher affinity for one of the lipid domain compositions. After incorporation of these molecules in the lipid bilayer, it is expected that an increase in the extent of lateral heterogeneity will result in a decrease of FRET efficiencies (E) when both donor and acceptor molecules segregate to different lipid domains (as this will result in an increase of the average distances between the two species in the membrane) and an increase of E values in the case of segregation of donors and acceptors to the same lipid domains (Fig. 1).

This approach was applied in its simplest form to the identification of phase coexistence during the gel-to-fluid transition of 1,2-dipalmitoyl-sn-glycero-3-phosphocholine (DPPC) (Pedersen et al. 1996). N-(7-nitrobenz-2-oxa-1,3-diazol-4-yl)-1,2-dihexadecanoyl-sn-glycero-3-phosphoe-thanolamine (NBD-DPPE) was chosen as the donor and the acceptor was N-(lissamine–rhodamine B sulfonyl)-1,2-dihexadecanoyl-sn-glycero-3-phosphoethanolamine (Rh-DPPE). In temperature scans of DPPC liposomes with identical concentrations of NBD-DPPE and Rh-DPPE (0.5 mol%), the fluorescence of NBD-DPPE peaked shar-ply at the main transition temperature (T_m) of DPPC. Because this peak was not observed in the absence of the acceptor it must be attributed to a decrease of energy transfer. These workers attributed this decrease to differ-ential segregation of the probes at T_m. The sensitivity of FRET to phase separation is even more remarkable when considering that the probe used in this study as the FRET donor had a partition coefficient between the gel and fluid phases of 1,2-lauroyl-sn-glycero-3-phosphocholine
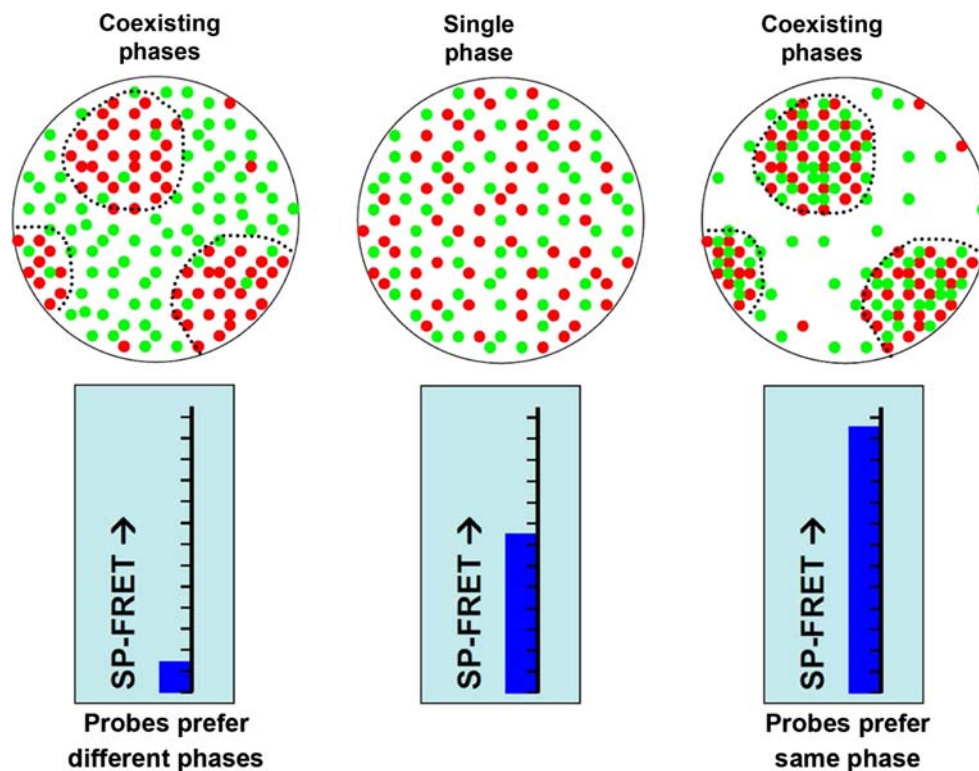
Fig. 1 Schematic representation of the effect of phase separation and probe partition on the FRET efficiency. D and A molecules are represented by *green* and *red* dots, respectively. In a single-phase membrane, an intermediate FRET signal intensity is observed. In the presence of coexisting phases, however, the probes can partition preferentially between alternative environments, causing their local concentrations to rise or fall. If the probes prefer different phases, they are effectively separated, reducing FRET. If the probes prefer the same phase, they are effectively clustered and the FRET signal increases. Reprinted figure with permission from Buboltz (2007), http://link.aip.org/link?pre/76/021903/pdf. Copyright 2007 by the American Physical Society

(DLPC)/1,2-distearoyl-sn-glycero-3-phosphocholine (DSPC) mixtures close to 1, i.e., affinities for the gel and fluid domains were almost identical in this binary system (Mesquita et al. 2000). Of course, the actual lipid composition can have a strong influence on probe partition (and not only the type of phases in coexistence; e.g., Baumgart et al. 2007). Still, one could cautiously interpret that the observed FRET variation reflects mostly changes in the distribution of the acceptor (rather than the donor) during the gel–fluid transition of DPPC in this experiment. Another possibility is that one of the probes has higher affinity for the interface between the gel and fluid domains, because this would also result in differential segregation of donors and acceptors during phase coexistence in the membrane (Leidy et al. 2001). This type of membrane distribution was verified for the fluorescent probe 1,1′-dioctadecyl-3-3-3′,3′-tetramethylindocarbocyanine (DiIC$_{18}$(3)) in a fluid/gel lipid bilayer (Loura et al. 2000b; see below).

Application of the same methodology with the same probes to a 1,2-dimyristoyl-sn-glycero-3-phosphocholine (DMPC)/DSPC mixture of lipids showed that FRET between NBD-DPPE and Rh-DPPE was also sensitive to phase coexistence in a binary mixture of lipids (Leidy et al.

2001). Interestingly, in this case two peaks were observed for the donor fluorescence in the heating profiles, each corresponding to the temperature boundaries for phase coexistence of DMPC and DSPC. For a binary mixture, phase separation was expected to induce only one minimum in E, corresponding to the situation of maximum probe segregation, expected to occur inside the phase coexistence range. The authors explain the observation of two peaks on the basis of trapped molecules in the DSPC-enriched gel phase, which do not experience segregation upon transition to the fluid phase of the low T_m lipid (DMPC). When the T_m of DSPC is achieved these trapped molecules are released and a second instance of probe segregation occurs.

Donor/acceptor pairs consisting of NBD/Rh-labelled phospholipids were shown to be generally highly sensitive to gel/fluid phase separation, but less so for fluid/fluid or lo/ld phase separation (Stilwell et al. 2000), reflecting the less distinct nature of the last two phases. In this work, energy transfer efficiencies were measured for given donor/acceptor FRET pairs at different Chol concentrations in liposomes with a ternary composition of Chol and equimolar concentrations of 1-stearoyl-2-oleoyl-sn-glycero-3-

phosphocholine and 1-stearoyl-2-docosahexaenoyl-*sn*-glycero-3-phosphocholine. The authors observed that E steadily increases as the Chol content increases and rationalized this as simultaneous partition of both donors and acceptors to the ld phase during phase separation. However, Chol produces a condensation effect on the lipid membrane (Smaby et al. 1997), and the ld phase presents larger areas per lipid than the Chol-enriched domains. In this case, it is expected that FRET efficiencies increase with an increase in the lo phase, even if the donor and acceptor probes have no preferential interaction with either lo or ld phases, as average distances between the FRET species decrease. Additionally, the fact that the variation of E is not monitored along a tie-line renders data interpretation very difficult.

Silvius (2003) presented a more accurate and sensitive approach to detection of membrane inhomogeneities by FRET. By comparing FRET efficiencies obtained with an acceptor with affinity for one of the lipid phases and two different donors which distribute to different membrane domains, changes in membrane area, or other properties relevant to FRET, will no longer lead to erroneous assumption of domain formation, because the changes in this case should affect both donor/acceptor pairs in an identical manner. When real deviations from heterogeneity are observed it is expected that the efficiencies of quenching for each donor will be affected in opposite ways. By applying this experimental design it was possible to identify domain formation in mixtures of sphingomyelin or saturated phospholipids and/or unsaturated phospholipids with physiological proportions of Chol (Silvius 2003; Fig. 2). Under identical conditions, previous studies using fluorescence microscopy techniques were not able to identify deviations to homogeneity (Dietrich et al. 2001; Veatch and Keller 2002), suggesting that the detected domains occurred at nanometer spatial scales.

Another possible artifact originating from FRET measurements in membranes is caused by neglecting fluctuations in donor and acceptor concentrations, which can lead to significant shifts in experimentally measured FRET efficiencies and an erroneous assumption of lipid domain formation. Changes in the lipid composition, temperature, or buffer properties can lead to dramatic changes in the partition coefficients of these molecules to the lipid membrane. Additionally, FRET donors and acceptors used in membrane studies often display high aqueous solubility that enable incorporation in the lipid membrane from aqueous solutions of the probe, and in these cases it is very likely that a significant number of molecules will not partition to the membrane. Determination of partition coefficients of fluorescent molecules to lipid membranes has been reviewed elsewhere (Santos et al. 2003). NBD-labelled phosphatidylinositol bisphosphate phospholipids
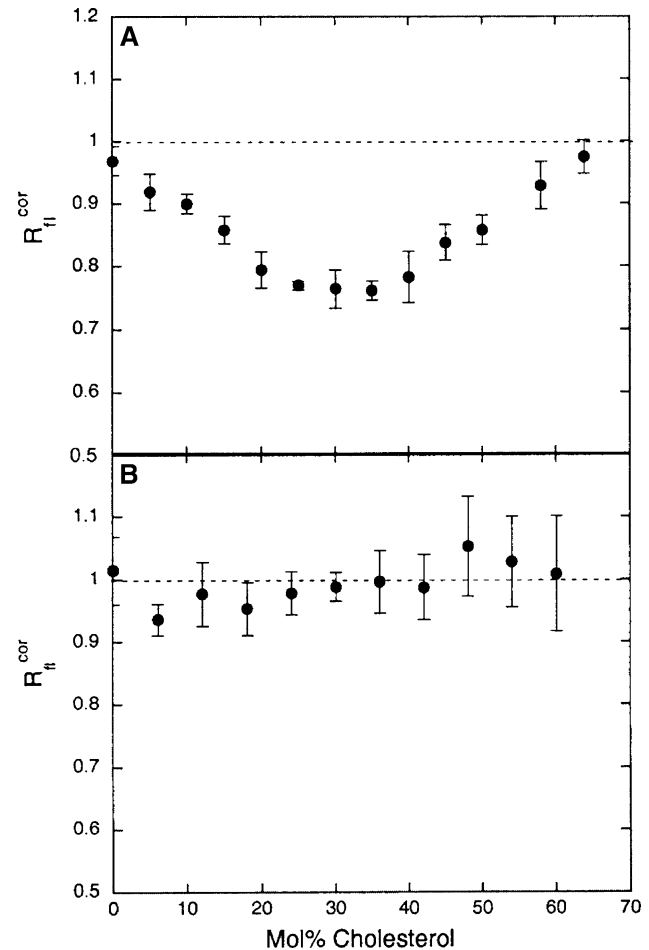

Fig. 2 Ratio of the FRET efficiencies measured for D = DONDO (an ld-preferring tetraoleoyl NBD phospholipid conjugate) relative to that measured for D = DSNDS (an lo-preferring tetrastearoyl NBD phospholipid conjugate) and for A = Rh-diphytanoyl PE (0.3 mol%), at 37°C, in mixed bilayers containing brain SM (**a** evidence for domain formation) or DOPC (**b** no domains are detected) with varying Chol content. Reprinted from Silvius (2003) with permission. Copyright 2003 Biophysical Society

(PIP$_2$) have been shown to partition to lipid membranes in a pH-dependent manner (Fernandes et al. 2006). This phenomenon is likely to be the cause of the observation, by use of FRET, of apparent fluid/fluid phase separation in PIP$_2$/phosphatidylcholine (PC) bilayers at or slightly above physiological pH (Redfern and Gericke 2004, 2005).

FRET in bilayers with uniform distribution of components

Förster resonance energy transfer theory was established by Theodor Förster (1949). The first-order rate coefficient of energy transfer from a directly excited donor species (D) to a suitable species (see below), the acceptor (A), is given by:

$$k_T = \frac{1}{\tau_0}\left(\frac{R_0}{R}\right)^6 \qquad (3)$$

where τ_0 is the D fluorescence lifetime in the absence of A, R is the D–A distance and R_0, commonly termed the Förster radius, depends on the relative orientation of D and A (through the so-called orientation factor, κ^2, discussed extensively by Van der Meer et al. 1994), the fluorescence quantum yield of D in the absence of A (Φ_0), the refractive index of the medium (n), and the overlap between the D normalized emission (I) and A absorption (ε) spectra according to:

$$R_0 = 0.2108\left[\kappa^2\Phi_0 n^{-4}\int_0^\infty \lambda^4 I(\lambda)\varepsilon(\lambda)\mathrm{d}\lambda\right]^{1/6} \qquad (4)$$

The constant value in the equation above assumes that nm and Å units are used for λ and R_0, respectively. It is clear that R_0 may be computed from spectral data of D and A, independently of the actual FRET experiment. The isotropic dynamic limit value (2/3) is generally assumed for κ^2. Typical values of R_0 lie in the 10–60 Å range for typical D/A FRET pairs.

Equation 3 is often used for the purpose of distance measurement on the R_0 scale, if R is the same for all D/A pairs. This condition is generally not met in membrane studies, for which D and A are randomly distributed in the bilayer, resulting in an impossibly large number of D/A distances. In this situation, if all donors are equivalent (uniform distribution of D molecules), one needs only to consider one D molecule. The decay rate constant for this selected donor, surrounded by N acceptor molecules, is given by:

$$k = \tau_0^{-1}\left[1 + \sum_{i=1}^N (R_0/R_i)^6\right] \qquad (5)$$

where R_i is the distance between the donor and the i-th acceptor molecule.

Equation 5 is the usual starting point for the derivation of D decay kinetics in membrane systems. Complex distributions, resulting, e.g., from distribution of D and A molecules in nanodomains, require the use of either simplified analytical treatments or numerical simulation, as described in the following section. Relatively concise analytical solutions have been derived for the simpler cases of acceptor uniform distribution in infinite planar media (Fung and Stryer 1978; Wolber and Hudson 1979). For two-dimensional D and A distribution, and admitting that the distance of closest approach between D and A, R_e, is much less than R_0 (in practice, if $R_e < 0.25R_0$), one obtains the following expression for the D decay in presence of A:

$$i_{DA}(t) = \exp(-t/\tau_0)\exp\left[-\pi\Gamma(2/3)R_0^2 c(t/\tau_0)^{1/3}\right]. \qquad (6)$$

In Eq. 6, Γ is the complete gamma function and c is the surface concentration of acceptors (A molecules per area unit). The first term on the right hand side corresponds to the decay of D in the absence of A, whereas the second term reflects the de-excitation because of the FRET interaction. Note that, whereas Eq. 5 implies that the decay of the donor surrounded by a finite number of acceptors is still exponential (albeit faster than in absence of acceptor), by taking the limit of infinite plane of acceptors the decay law becomes complex. The FRET term, proportional to $t^{1/3}$, dominates at early times and vanishes for $t/\tau_0 \gg 1$. This leads to a characteristic shape of the decay curve, very fast at the beginning, and becoming asymptotically parallel to that in the absence of A for longer times (Fig. 3; note that the decays are strictly parallel only for very long times, $t > 10\tau_0$. For this reason, and because of the cut-off in the y-axis for low photon counts, this limit behaviour is only hinted at in the figure).

If R_e is not negligible relative to R_0, the decay law becomes somewhat more complex:

$$i_{DA}(t) = \exp\left(-\frac{t}{\tau_0}\right)\exp\left\{-\pi R_0^2 n\gamma\left[\frac{2}{3},\left(\frac{R_0}{R_e}\right)^6\left(\frac{t}{\tau_0}\right)\right]\left(\frac{t}{\tau_0}\right)^{1/3}\right\}$$
$$\cdot \exp\left\{\pi R_e^2 n\left(1 - \exp\left[-\left(\frac{R_0}{R_e}\right)^6\left(\frac{t}{\tau_0}\right)\right]\right)\right\} \qquad (7)$$

In this equation, γ is now the incomplete gamma function. Although it was originally derived for a plane of acceptors
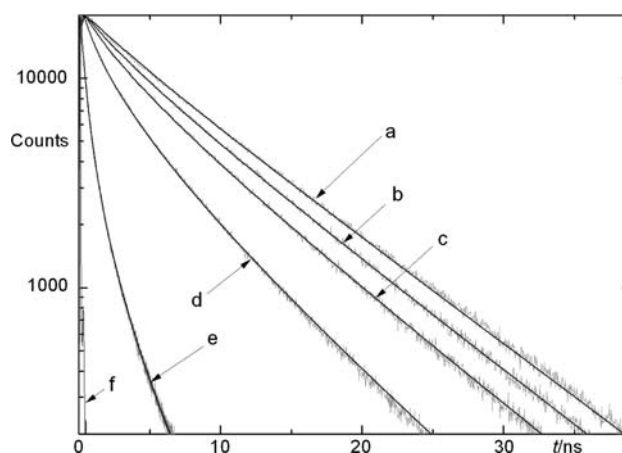

Fig. 3 Typical decays of a bilayer-inserted donor species (D = 1,6-diphenylhextriene, DPH) undergoing FRET to membrane-bound acceptors (A = 1-palmitoyl-2-[6-NBD-aminohexanoyl]-*sn*-glycero-3-phosphocholine). Membrane system: fluid DPPC (50°C). D:total lipid = 1:500. A:total lipid = 0 (*a*), 1:400 (*b*), 1:167 (*c*), 1:64 (*d*), 1:16 (*e*). The pulse profile of the excitation laser light is also shown (*f*). The *grey lines* are experimental decays, and the *black smooth lines* are the fits to the model of uniform probe distribution

containing the donor (*cis* transfer), it is also valid if the D molecule is separated from the A plane by a distance R_e, a situation common on membranes, because D and A are often located at different depths in the bilayer (*trans* transfer). A different derivation of the decay law in this geometrical arrangement is given by Davenport et al. (1985).

Upon preparation of lipid vesicles, D and A molecules are frequently inserted in either of the bilayer leaflets, with equal probability. In this case, one must consider two planes of acceptors for a given donor, one corresponding to the acceptors lying in the same bilayer leaflet as the donor, and another for those located in the opposite leaflet. The decay law in this case is obtained by simply multiplying the intrinsic donor decay by the FRET terms corresponding to each plane of acceptors.

Another common occurrence in membrane systems is complex decay of the donor even in the absence of acceptors, with a sum of two or three exponentials being required for proper description. In this case, the above equations can be still used if the exponential donor intrinsic decay term is replaced by this function and τ_0 is replaced by the intensity-average decay lifetime.

Whereas in earlier applications of the uniform distribution formalism to one-component bilayers the objective was to verify the applicability of Förster FRET theory to model membranes (Fung and Stryer 1978; Loura et al. 1996, 2000a), nowadays its main utility is as a test of whether the addition of a new component to a given one-phase lipid bilayer system induces compartmentalization and/or phase separation. This would be detected in the failure to analyse FRET kinetics with uniform probe distribution formalisms. Recent examples of this kind include a study that demonstrated the absence of clustering of phosphatidylinositol-4,5-bisphosphate (PI(4,5)P$_2$) in a fluid PC matrix at slightly above physiological pH, following the satisfactory description of FRET between 1,6-diphenylhexatriene (DPH) and NBD-labelled PI(4,5)P$_2$, in 1-palmitoyl-2-oleoyl-*sn*-glycero-3-phosphocholine (POPC) vesicles with 5 mol% of total PI(4,5)P$_2$ (Fernandes et al. 2006) at pH 8.4. On the other hand, time-resolved FRET between the tryptophan residues of acetyl-GWW(LA)$_8$ LWWA-amide peptide (WALP23) and the fluorescent Chol analog dehydroergosterol (DHE), both with and without added equimolar amounts of Chol, could be satisfactorily globally analysed assuming uniform DHE distribution in the bilayer (Holt et al. 2008). This FRET pair (tryptophan/DHE) was also used in a study of the hypothetical affinity of the γM4 peptide from the muscle acetylcholine receptor (donor: Trp453) for Chol (acceptor: DHE) in the lo phase of POPC/Chol. The measured FRET efficiencies were significantly lower than expected, which

was interpreted on the basis of formation of peptide-rich, sterol-depleted patches (de Almeida et al. 2004). Higher FRET efficiency than expected was observed between M13 major coat protein labelled with *n*-(iodoacetyl) aminoethyl-1-sulfonaphthylamine (IAEDANS, donor) and *n*-(4,4-difluoro-5,7-dimethyl-4-bora-3*a*,4*a*-diaza-*s*-indacene-3-yl)methyl iodoacetamide (BODIPY, acceptor) in supposedly monophasic (fluid) bilayers of 1,2-dierucoyl-*sn*-glycero-3-phosphocholine/1,2-dioleoyl-*sn*-glycero-3-phosphocholine (DOPC) and 1,2-dimyristoleoyl-*sn*-glycero-3-phosphocholine/DOPC, because of formation of domains enriched in the protein and the matching lipid (DOPC; Fernandes et al. 2003).

Sometimes addition of a component leads to changes in FRET efficiency that are not related to phase separation, but to other morphological changes in the organization of the lipid. This was the case in recent studies of mixed PC/anionic lipid (phosphatidylserine, PS) vesicles incubated with a basic peptide (K$_6$W; Loura et al. 2006) or protein (lysozyme; Coutinho et al. 2008), where formation of stacked lipid multilayers, bridged by peptide or protein, was concluded. Whereas the observed FRET efficiency variations could be due to either lateral demixing or multilayer formation, global analysis of time-resolved data can clearly distinguish between the two situations. In the studies mentioned, no significant lateral phase separation takes place. The variations in the extent of FRET result from multilayer formation, and it was even possible to measure the spacing repeat distance in these structures.

The uniform distribution formalism is also the starting point for related models which incorporate the possibility of donor–acceptor aggregation. This is often applied to the study of protein/peptide oligomerization (the species under study is labelled with either donor or acceptor fluorophores, which are then incorporated into bilayers in different proportions). In this case, two types of FRET are operative—highly efficient intra-aggregate FRET and "background" intermolecular FRET (often neglected in early models; Adair and Engelman 1994; Li et al. 1999). This rationalization recently enabled us to conclude that the N-BAR N-terminal domain forms antiparallel dimers in 1-palmitoyl-2-oleoyl-*sn*-glycero-3-phosphoglycerol vesicles (Fernandes et al. 2008).

A novel use of the uniform distribution formalism is the quantification of the extent of interaction of a peptide with membranes, in cases when the intrinsic fluorescence behaviour of the peptide is not altered upon binding to the bilayer. This has recently been illustrated for the HIV-1 fusion inhibitor peptides T-1249 (Veiga et al. 2004) and sifuvirtide (Franquelim et al. 2008) in POPC/Chol lo and DPPC gel phases, respectively.

FRET in phase-separated bilayers

Infinite phase separation

Now we consider specifically the situation of phase separation. In this case, both D and A will distribute between the coexisting phases. This distribution will affect the FRET efficiency relative to the uniform distribution case, increasing it if D and A prefer the same phase or decreasing it if the two probes prefer distinct phases (Fig. 1). Let us assume that D molecules inside phase i ($i = 1, 2$) are only capable of transferring energy to A molecules inside the same phase (intraphase FRET exclusively, no interphase FRET). This situation is met in the limit of large domains (domain size $\gg R_0$), for which boundary effects are negligible, and is termed the infinite phase separation case. The donor decay is simply a linear combination of the decay in each phase, weighed by the fraction of D molecules in phase i (A_i, $i = 1, 2$):

$$i_{\mathrm{DA, phase\ separation}}(t) = A_1 i_{\mathrm{DA, phase\ 1}}(t) + A_2 i_{\mathrm{DA, phase\ 2}}(t) \quad (8)$$

The functions $i_{\mathrm{DA}}(t)$ are calculated using the equation pertinent to each particular situation. In general, the surface concentration of A (c_i), the closest D/A approach distance (R_{ei}) and the lifetime of D in absence of A (τ_i) will differ between the two phases. It is clear that the number of fitting terms increases significantly upon phase separation, and meaningful recovery demands the use of global analysis, that is, simultaneous analysis of the DA and the D decays, with linkage of the common terms, A_2/A_1, τ_1 and τ_2.

Equation 8 (or the integrated form after substituting into $i_{\mathrm{DA}}(t)$ in Eq. 2) has been used to analyse FRET in biphasic bilayers with either gel/fluid (Loura et al. 2000b, 2006; de Almeida et al. 2002) or lo/ld (Loura et al. 2001a, b; de Almeida et al. 2005) phase coexistence, in order to gain insight on the size of the existing domains. A general conclusion of these studies is that good statistical description of the experimental decays by Eq. 8 does not guarantee the validity of the infinite phase hypothesis. However, the latter can be conveniently assessed by examining the recovered values of A_i and c_i, and comparing these with the values expected from consideration of the probe partition equilibria, as described in the following subsections.

Probe partition, phase boundaries, and FRET

The distribution of molecules of a given species between the two coexisting phases 1 and 2 of a biphasic membrane system is usually described in terms of a partition equilibrium:

$$(\mathrm{probe})_1 \leftrightarrows (\mathrm{probe})_2 \quad (9)$$

which is characterized by the partition coefficient, defined as (Davenport 1997):

$$K_{\mathrm{p}} = (P_2/X_2)/(P_1/X_1) \quad (10)$$

where P_1 is the probe mole fraction in lipid phase 1, and X_1 is the mole fraction of lipid phase 1 (with $P_2 = 1 - P_1$ and $X_2 = 1 - X_1$). Equations 8 and 10 can be combined, to yield convenient expressions for the partition coefficients of both D (K_{pD}) and A (K_{pA}) (Loura et al. 2001b):

$$K_{\mathrm{pD}} = (A_2/X_2)/(A_1/X_1) \quad (11)$$

$$K_{\mathrm{pA}} = (c_2 a_2)/(c_1 a_1) \quad (12)$$

where a_i is the area per lipid molecule in phase i.

We now show that the composition/temperature (x, T) phase diagram boundaries (x_1 and x_2, corresponding to pure 1 and 2 phases, respectively) can also be obtained from the time resolved FRET parameters, in the framework of the infinite phase separation hypothesis (Loura et al. 2001b). Let F be the overall A mole fraction, and F_i be the A mole fraction within phase i. The latter is related to c_i according to:

$$F_i = c_i a_i \quad (13)$$

Following computation of F_i, from the acceptor mass balance equation:

$$F = F_2(1 - X_1) + F_1 X_1 \quad (14)$$

calculation of X_1 and X_2 is straightforward, even for an unknown phase diagram. If this is carried out for two points, A(x_{A}, T) and B(x_{B}, T), and combined with the lever rule, one obtains the following simple expressions for the phase boundaries:

$$x_1 = (x_{\mathrm{A}} X_{2\mathrm{B}} - x_{\mathrm{B}} X_{2\mathrm{A}})/(X_{1\mathrm{A}} - X_{1\mathrm{B}}) \quad (15)$$

$$x_2 = (x_{\mathrm{B}} X_{1\mathrm{A}} - x_{\mathrm{A}} X_{1\mathrm{B}})/(X_{1\mathrm{A}} - X_{1\mathrm{B}}) \quad (16)$$

If this procedure is repeated for several temperatures, the phase diagram is obtained.

More recently, Buboltz (2007) developed a new experimental approach ("steady-state probe-partitioning FRET" or SP-FRET) for characterization of phase separation in lipid membranes that relies solely on acceptor steady-state sensitized emission. The procedure requires measurements with different FRET pairs exhibiting complementary partitioning (Fig. 1, left), i.e., at least one of the FRET species employed should be preferentially enriched in each of the coexisting lipid phases. Sensitized emissions in each phase are expressed as a function of local D and A mole fractions, and two constants including all photophysical effects in the respective phase. On the low acceptor concentration regime this relationship was significantly simplified (Buboltz et al. 2007a). Fitting of this model to the sensitized fluorescence data, together with prior specification of the position of tie-lines and phase boundaries of the lipid system under study, enables determination of the probes' interphasic partition

coefficients as the sole fitting properties. Information on the phase boundaries can be obtained from the detection of the lipid compositions for which the gradient of sensitized acceptor emission relative to composition was maximum. One important assumption in this method is that no FRET events occur between molecules located in different phases, i.e., R_0 values are much smaller than the average lipid domains (this can be achieved by selection of donor/acceptor FRET pairs with small spectral overlap) and the infinite phase approximation is taken. Therefore, this method is a tool to probe phase boundaries, but not domain sizes. The author successfully applied this approach to the study of gel/fluid phase separation in DLPC/DSPC mixtures by globally fitting data obtained from two different combinations of donor/acceptor pairs. The need for multiple donor/acceptor pairs is a consequence of the degeneracy of the model with regard to the partition coefficients of the probes in each set of measurements.

In another study, the same methodology for detection of phase boundaries was used for the characterization of the DOPC/DPPC/Chol lipid mixture (Buboltz et al. 2007b). Fluorescence data from 1294 independently prepared samples were analysed and phase boundaries were obtained from the gradients of acceptor sensitized emission from 3,3′-dioctadecyloxacarbocyanine (18:0-DiO), using DHE as the FRET donor. Three different regions of phase coexistence were clearly identified (gel/fluid, lo/ld, and lo/Chol crystals), showing some differences from results from confocal fluorescence microscopy (CFM) and solid-state NMR studies (Veatch and Keller 2003; Veatch et al. 2004). Notably, the lo/ld coexistence range is narrower at room temperature (not extending beyond 33 mol% Chol, compared with 50 mol% for the confocal fluorescence microscopy boundary). Also, as the temperature increases, coexistence in that region extends in its entirety to higher DPPC content, whereas for CFM measurements only the ld boundary is affected. The authors attribute this discrepancy to the use of a different methodology in sample preparation. CFM and solid-state NMR require film deposition of lipid to produce giant unilamellar vesicles or oriented membranes, and this might result in increased susceptibility to demixing of lipid components, whereas in this study, polydisperse multilamellar vesicle suspensions were prepared by the rapid solvent-exchange method, which does not require formation of this intermediate lipid film. Interestingly, two other studies on this ternary system were recently published, neither of which restricted to giant unilamellar vesicles. De Almeida et al. (2007), using a combined time-resolved fluorescence microespectroscopic approach (that is, fluorescence lifetime-imaging microscopy and microscopic fluorescence decays measured in giant unilamellar vesicles, and macroscopic fluorescence decays measured in large unilamellar vesicles), established

the existence of the three-phase triangle near the palmitoyl/palmitoyl corner, thus narrowing the lo/ld previously reported (Veatch et al. 2004). In the same year, a NMR study of multilamellar vesicles by Veatch et al. (2007) indicated that lo/ld coexistence region does not extend beyond 35 mol% Chol for 10–37°C.

Detection of nanodomains from deviations to infinite phase separation

If nanodomains (that is, domains of size of the order of R_0) are formed, the infinite phase separation condition is no longer justified, as donors near the domain boundaries can transfer excitation energy to acceptors both inside and outside the domains. Derivation of an analytical solution to this problem remains unsolved (see the section "Analytical formalisms for estimation of domain size" for approximate analytical solutions). One approach involves applying Eqs. 8, 11–12, and 15–16, strictly valid only for infinite phase separation, to the analysis of FRET time-resolved data. This was tested using synthetic decays generated by numerical simulation of the FRET kinetics for probe distribution in domains of size ~ 3.5–$4\,R_0$ and ~ 9–$10\,R_0$, that is ~ 18 nm and ~ 45 nm, respectively, for a typical $R_0 = 5$ nm value (Loura et al. 2001b; see the following subsection). Input values were chosen for x, x_1, x_2, K_{pD} and K_{pA} (from which X_1, X_2, c_1 and c_2 were obtained using the equations presented above). It was verified that statistically acceptable fits were obtained for all simulations (global $\chi^2 < 1.1$). For domains of $\sim 10\,R_0$ size the values of c and K_{pA} recovered after analysis of the synthetic decays are very similar to the input simulation values (meaning that domains $>10\,R_0$ are virtually indistinguishable from infinite phases from the FRET point of view). In contrast, noticeable differences were observed between the input and recovered c_1 and c_2 values for the smaller domains. In these cases, the highest c value is always underestimated, whereas the lowest c value is consistently overestimated. This is because of the small domain size—many of the donors located in phase 1 are sensitive to acceptors in phase 2, and conversely for the donors located in phase 2. This effect is more pronounced for the domain phase than for the continuous phase, especially when the former is more abundant. As a consequence of these deviations, the K_{pA} values are always closer to unity than expected. From this study, a procedure for obtaining information about the size of membrane domains was proposed (Loura et al. 2001b):

(1) measure K_{pA} by methods insensitive to the size of the underlying domains (e.g., from the variation of fluorescence intensity, lifetime, or anisotropy along the tie-line);

(2) obtain time-resolved FRET data and calculate K_{pA} from global analysis;

(3) compare the K_{pA} values obtained in (1) and (2) and, from their eventual difference, come to a conclusion about domain sizes;

(4) this would allow an "educated guess", which could, in turn, be confirmed by appropriate numerical simulations (following subsection). Theoretical decay laws would thus be obtained and compared with the experimental ones.

Because lipid mixtures exhibiting gel/fluid heterogeneity were better characterized from the equilibrium point of view, these were the first biphasic systems to be studied by FRET in the framework of the infinite phase separation formalism. In 2000, a report of the DLPC/DSPC system was published (Loura et al. 2000b). The donor was a short acyl-chain head-labelled phospholipid, N-NBD-dilauroylphosphatidylethanolamine (NBD-DLPE), and two identical carbocyanine acceptors were used, differing solely in the aliphatic chain length, 1,1′-didodecyl-3,3,3′,3′-tetramethylindocarbocyanine (DiIC$_{12}$(3)), and DiIC$_{18}$(3). From hydrophobic matching (Mouritsen and Bloom 1984) arguments, the C$_{12}$-chain probes NBD-DLPE and DiIC$_{12}$(3) were expected to prefer the C$_{12}$-lipid (DLPC)-rich fluid phase, whereas it was expected that the C$_{18}$ acceptor DiIC$_{18}$(3) would preferentially be located in the C$_{18}$-lipid (DSPC)-rich gel phase. This was indeed observed from the partition coefficients obtained from variation of steady-state anisotropy (NBD-DLPE) and fluorescence lifetime (DiIC$_{12}$(3), DiIC$_{18}$(3)) along the phase diagram tie-lines at 22 and 40°C, and agrees with the FRET results for the NBD-DLPE/DiIC$_{12}$(3) pair. However, the NBD-DLPE/DiIC$_{18}$(3) pair tells a different story, and K_{pA} calculated from Eq. 12 was unexpectedly indicative of preference for the fluid phase. These apparently conflicting results were rationalized on the basis of segregation of DiIC$_{18}$(3) to the interface between gel and fluid domains, where the probe would essentially act as a surfactant, reducing the interfacial tension and stabilizing a nanodomain structure. The same system was later studied using the gel-phase probe trans-parinaric acid (t-PnA) as donor and NBD-DLPE as acceptor (de Almeida et al. 2002). For this pair, phase separation leads to a decrease in the measured FRET efficiency (indicating increased D/A separation, in agreement with the expected probe partition preference), and the equilibrium value of the latter agrees with the theoretical expectation for infinite phase separation. In this case, t-PnA distributes uniformly inside the gel phase, and no interface effects are apparent at equilibrium. Because there is a large driving force for gel/fluid phase separation upon cooling a binary mixture with large hydrophobic mismatch, this process is expected to proceed

to completion and no small domains should be present at equilibrium. This behaviour was observed in Monte-Carlo simulation studies (Jørgensen and Mouritsen 1995) and agrees with the above described FRET study.

This was also verified for the DPPC/1,2-dipalmitoyl-sn-glycero-3-phosphoserine (DPPS; anionic phospholipid) equimolar mixture at 45°C (gel/fluid phase separation; Loura et al. 2006). In this study, FRET decays of 1-palmitoyl-2-[3-(diphenylhexatrienyl)propanoyl]-sn-glycero-3-phosphocholine (DPH-PC; FRET donor) were measured in the absence and presence of 1-palmitoyl-2-[12-NBD-aminododecanoyl]-sn-glycero-3-phosphocholine (NBD-PC; FRET donor), for varying concentrations of the basic peptide hexalysyltryptophan (K$_6$W). It was intended to study whether the presence of peptide led to changes in the lipid organization, namely regarding the size of the domains. From variation of the NBD-PC lifetime, a size-independent partition coefficient of $K_{pA}^{g/f} = 0.31 \pm 0.06$ was obtained. Addition of peptide does not lead to significant change in the $K_{pA}^{g/f}$ calculated from the FRET data, and a nonmonotonic variation is observed, with $K_{pA}^{g/f} = 0.20 \pm 0.09$. The lack of systematic variation of $K_{pA}^{g/f}$ on increasing the concentration of K$_6$W indicates inability of the peptide to change appreciably the domain organization in this system. The fact that the FRET and non-FRET $K_{pA}^{g/f}$ values agree (and, in particular, the FRET value is not closer to unity relative to the non-FRET value) indicates that domains are large on the FRET scale.

Ld/lo phase separation differs from the gel/fluid case in that the coexisting phases are more similar in nature. Additionally, there is evidence that Chol molecules (at least in ternary systems containing sphingomyelin (SM)) may accumulate to some extent in the domain boundaries, thus reducing the interfacial tension (Brown 1998; Pandit et al. 2004; London 2005). This could help stabilize nanodomain formation, which in turn leads to a favourable concomitant entropic increase. Thus, phase separation is not necessarily expected to proceed to completion in these systems. To investigate this hypothesis, time-resolved FRET measurements were carried out for DMPC/Chol mixtures above the phospholipid T_m (Loura et al. 2001b). The FRET donor used was N-NBD-dimyristoylphosphatidylethanolamine (NBD-DMPE) whereas the acceptor was N-(lissamine–rhodamine B)-dimyristoylphosphatidylethanolamine (Rh-DMPE). These probes have opposite phase preference in this system, as seen from the $K_p^{lo/ld}$ recovered using fluorescence data insensitive to domain size (fluorescence anisotropy and intensity, respectively; Table 1). Therefore, as a result of domain formation, a decrease in FRET efficiency is observed (Fig. 1, left, and Fig. 4). D decays were recorded and globally

analysed for three compositions ($x_{Chol} = 0.15$, 0.20 and 0.25) inside the reported phase coexisting range (Almeida et al. 1992; Mateo et al. 1995). Interestingly, this decrease is very small for low X_{lo}, and only when lo is the majority phase (high x_{Chol} inside the phase coexistence range) does the FRET efficiency decrease significantly.

Table 1 compares the FRET-recovered $K_p^{lo/ld}$ with the "non-FRET" values. As described above, $K_{pA}^{lo/ld}$ closer to unity relative to the "non-FRET" value indicates that the formed domains are small in size. In accordance to the FRET efficiency variation commented above, this is the case for the compositions for which ld is the majority phase, namely $x_{Chol} = 0.15$. It is interesting to compare the relative deviations between the FRET-recovered K_{pA} and the theoretical values (for the simulations) or the fluorescence intensity-recovered values (for the experimental study). From the numerical simulation, the average relative deviation in K_{pA} is 27% for domains of size ~ 3.5–$4\,R_0$ and 10% for domains of size ~ 9–$10\,R_0$. The deviations for the experimental study are 143% (30°C, $x_{Chol} = 0.15$), 40% ($T = 30$°C, $x_{Chol} = 0.20$), 74% ($T = 40$°C, $x_{Chol} = 0.15$), and 81% ($T = 40$°C, $x_{Chol} = 0.20$).

These numbers should be viewed cautiously, because there is not exact matching between input simulation variables and the experimental parameters, and the simulated domains had a shape and size distribution that probably differs from the actual ones, but they clearly indicate that lo domains smaller than ~ 3.5–$4\,R_0$ (~ 18 nm) form for $x_{Chol} = 0.15$ and 0.20 in this system. On the other hand, the FRET $K_{pA}^{lo/ld}$ values are actually somewhat lower (further from unity) than the fluorescence intensity values when lo is the majority phase ($x_{Chol} = 0.25$), meaning that extensive (on the FRET scale) phase separation occurs at this end of the tie-line.

A similar dependence of domain size on the amount of lo phase was observed for more complex systems, such as

Table 1 Comparison of K_p (lo/ld) values of D = NBD-DMPE and A = Rh-DMPE in DMPC/Chol mixtures obtained from FRET global decay analysis (second, third, and fourth columns) with those obtained from variations of fluorescence anisotropy (K_{pD}) or fluorescence intensity (K_{pA})

	$x_{chol} = 0.15$	$x_{chol} = 0.20$	$x_{chol} = 0.25$	Values from r or I_F
30°C				
K_{pD}	1.1	1.5	1.2	1.1
K_{pA}	0.73	0.42	0.18	0.30
40°C				
K_{pD}	1.5	3.2	2.6	2.6
K_{pA}	0.47	0.49	0.20	0.27

Reprinted with permission from Loura et al. (2001b). Copyright 2001 Biophysical Society

the raft model ternary system palmitoyl-SM (PSM)/POPC/Chol. Again, small domains were identified when $X_{lo} < 0.35$, as the efficiency of FRET between the lo-preferring donor, NBD-DPPE, and the ld-preferring acceptor, N-(lissamine–rhodamine B)-dioleoylphosphatidylethanolamine (Rh-DOPE) was almost invariant (de Almeida et al. 2005). For high X_{lo}, a steep drop in E, to significantly lower values than those observed in the binary DMPC/Chol system, was verified. This was interpreted as revealing that the domains formed at the high lo end of the studied tie-line (the end containing the 1:1:1 composition) were larger than those in the binary system. This agrees with the fact that ld/lo phase separation in binary mixtures, albeit well documented in the literature, has not been observed using fluorescence microscopy, in contrast with ternary mixtures (discussed in full by de Almeida et al. 2005). By measuring the variation of FRET efficiency along a tie-line of the phase diagram, as a function of X_{lo}, the effects of addition of small amounts of raft marker ganglioside G_{M1}, cholera toxin subunit B (de Almeida et al. 2005), and N-palmitoylceramide (Silva et al. 2007) have been studied.

Numerical simulations of FRET in heterogeneous membrane systems

One way to tackle the complexity of the FRET kinetics in nano-heterogeneous membrane systems is to calculate the D decay using numerical simulation. The concept is rather simple:

1. The topology of the lipid matrix is built. This means that, after choosing the size of the simulated system, domain shape, average size, and size distribution (monodisperse/polydisperse), the domains are randomly placed in the bilayer, in order to ensure that the overall fraction of each phase is as intended.
2. The D and A probes are placed in the system, according to their partition preferences. In practice, one chooses the total number of donor and acceptor molecules (to yield the desired overall probe:lipid ratios), calculates the number of probe molecules in each phase from the partition coefficients, and then randomly places each probe molecule. To this effect, the in-plane coordinates of a given probe molecule are randomly generated and checked to ensure its location either inside or outside the domains. Both lattice and off-lattice models can be used.
3. For each time t, the ensemble-averaged D excitation probability is computed. This is done by selecting a given D molecule, for which the decay rate constant is calculated using Eq. 5. The distance between this donor and all A molecules is calculated from the coordinates previously obtained. If D and A have
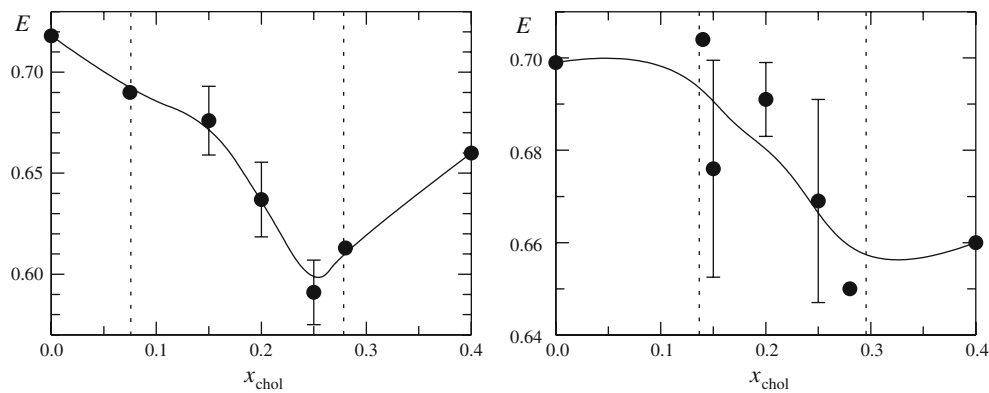
Fig. 4 Variation of FRET efficiency of NBD-DMPE (0.1 mol%)/Rh-DMPE (0.5 mol%) in DMPC/Chol LUV, as a function of Chol mole fraction, for $T = 30°C$ (**a**) and $T = 40°C$ (**b**). The *error bars'* extremes are the results of two different measurements. The *dotted* *vertical lines* represent the phase coexistence limits. Reprinted from Loura et al. (2001b) with permission. Copyright 2001 Biophysical Society

different transverse coordinates, this is obviously taken into account in the distance calculation. The summation in Eq. 5 is extended either to all acceptors in the system or to those within a cut-off distance of the selected donor. The probability is then calculated and averaged for all donors in the system.

4. If the simulated decay is intended to test an analytical model, it is convoluted with an experimental instrument response function, and Poisson noise is then added. Otherwise, if one wishes to obtain the theoretical FRET efficiency, time integration is carried out using Eq. 2.

Numerical simulations have already been described by Wolber and Hudson (1979) for uniform distribution in a planar geometry to test their analytical theory. The first numerical solution of FRET for non-uniform membrane probe distribution was given by Snyder and Freire (1982). These authors calculated FRET efficiency curves in planar systems as a function of acceptor concentration for uniform and non-uniform probe distribution and varying exclusion distance, and fitted simple analytical expressions (convenient for analysis of experimental data) to their numerical results. Heterogeneity of probe distribution is introduced by incorporating a heuristic potential function in the random placement of the probes. Therefore, no domains are actually simulated, and whereas the authors' equations are suited to analysis of probe aggregation in a single phase system, they are not useful regarding phase separation.

Simulations in which probe distribution heterogeneity is introduced by building a biphasic system and taking into consideration probe partition have been presented by Loura and coworkers (Loura and Prieto 2000; Loura et al. 2001b) and Towles and coworkers (Towles et al. 2007; Towles and Dan 2007). In both cases, the simulations were used to test the authors' analytical models and not with the intention of providing fitting equations as done by Snyder and Freire.

This is easily understood, noting that there are too many parameters to be accommodated by a useful fitting scheme. Whereas in the Snyder and Freire simulations the fitting parameters were the acceptor reduced concentration (acceptors per R_0^2), the exclusion distance, and an interaction parameter, the last of these would be replaced by a large set of variables (domain size and size distribution, domain shape, fraction of each phase, donor and acceptor partition coefficients).

In the simulations described above, just as in the analytical models described thus far, it is assumed that all acceptors are available to quench a given donor (the sum in Eq. 5 is extended to all acceptors). This approximation is valid if the number of excited acceptors is so low that their steady-state concentration is small compared with the total concentration of molecules. A convenient way to avoid this complication is to recreate the excitation and de-excitation processes of each D or A molecule by performing stochastic simulations. These calculations take into account the probabilities of donor excitation (equal for every unexcited donor at each time step), donor decay by non-FRET processes (given, in the absence of acceptors, by the ratio between the duration Δt of each time step and τ_0), FRET to any acceptor (overall, the probability of de-excitation of an excited donor in presence of acceptors is given by $\Delta t(1/\tau_0 + k)$, where k can be calculated by use of Eq. 5 and the sum therein excludes acceptor molecules in the excited state; the particular acceptor molecule which becomes excited is selected weighing the individual k_T rates (given by Eq. 3) of all potentially suitable acceptors), and acceptor de-excitation (given by the ratio of Δt to acceptor lifetime). The FRET efficiency is simply calculated by use of the ratio of the total number of transfers to the total number of donor excitations. This type of simulation is particularly useful in the simulation of energy migration between identical molecules (homo-FRET), because of the crucial possibility of

return of excitation to a previously directly excited donor, which implies the necessity of keeping track of excitonic location in this case (Demidov 1999). More recently, applications to hetero-FRET in planar geometries of similar algorithms have been published (Frederix et al. 2002; Berney and Danuser 2003; Corry et al. 2005). Kiskowski and Kenworthy (2007) used this approach to calculate the dependence of FRET efficiency on acceptor concentration for a planar geometry with disk-like domains. Two scenarios were considered: co-localization of donors and acceptors inside the domains; and segregation of acceptors to the other phase, with donors inside the domains. The authors showed that the local acceptor concentration inside the domains (and hence the domain fractional area) could be recovered from the first type of probe distribution, unlike the domain radius. However, the latter could be estimated from the acceptor segregation scenario, namely for small and intermediate-sized domains.

Obviously, similarly to the other treatments described above, this study cannot provide, by itself, a way to analyse experimental data directly, as many degrees of freedom are expected in an actual experiment. The authors fix values for R_0, donor–acceptor exclusion distance, domain radius, and donor and acceptor lifetime. Two extremely important degrees of freedom remain unconsidered, the donor and acceptor partition coefficients. The authors chose to study the extreme situations of co-localization inside the domains (corresponding to domain/continuous phase partition coefficients $K_{pD} = K_{pA} = \infty$) and total acceptor segregation ($K_{pD} = \infty$, $K_{pA} = 0$). These all-or-nothing scenarios led to maximal sensitivity in the recovery of the desired parameters. To model the effect of physical finite K_p values, simulations in which the probes are distributed taking them into account must be performed. It is clearly expected that distribution of D and A probes between the two phases will blur the method sensitivity to the desired parameters. Still, the use of the stochastic simulation algorithm constitutes an interesting variation in modelling FRET in heterogeneous membrane systems, and the illustrative calculations and analyses provide a simple guideline for experiments: pairs with large K_{pD} and K_{pA} are suited to estimation of the domain fraction; pairs with large K_{pD} but small K_{pA} should be useful for probing domain size.

An altogether different approach was recently used in a study of brain SM (BSM)/POPC/Chol. This was based on a combination of FRET (between 1-[[(6,8-difluoro-7-hydroxy-4-methyl-2-oxo-2H-1-benzopyran-3-yl)acetyl]oxy] (Marina Blue)-labelled and NBD-head-labelled 1-palmitoyl-2-oleoyl-sn-glycero-3-phosphoethanolamine (POPE)) and statistical mechanical lattice Monte-Carlo simulations (Frazier et al. 2007). For the purpose of FRET efficiency calculation from the simulations, the actual distance dependence of the FRET interaction was replaced by a step

function, meaning that FRET was considered to occur if the donor–acceptor distance in a given pair was less than R_0 (4.6 nm). With this simplification, and using unlike nearest-neighbor interaction parameters (the only potential fitting parameters in their Monte-Carlo methodology) based on experimental data (and fine-tuned by comparison with the experimental FRET, see Fig. 5a), the authors were able to observe extensive phase separation for a BSM/Chol/POPC mole ratio 35:35:30 (Fig. 5b). This agrees with the results of de Almeida et al. (2005) described above, which indicate the existence of large ld domains in this lo-rich area of the phase coexistence range. No extensive phase separation is observed in the Monte-Carlo simulation of any of the binary mixtures BSM/POPC 70:30, Chol/POPC 70:30, or BSM/Chol 50:50, which, as argued by the authors, agrees with the lack of observation by fluorescence microscopy in giant unilamellar vesicles of micron-scale phase separation in the binary SM/Chol, SM/POPC, and Chol/POPC systems, unlike some ternary mixtures of these components. This work demonstrates that FRET and computational techniques can be combined to create a powerful combination, suited to the study of lipid phase separation.

Analytical formalisms for estimation of domain size

As stated above, no exact solution of the FRET rate or efficiency has been derived for incomplete phase separation with nm-sized domains of a given type dispersed in the continuous phase. This stems from the evident symmetry loss introduced by the presence of the domains. For example, a donor located in the continuous phase will sense acceptors located both in the same phase and inside the domains. The distances between the latter and the selected donor depend on the domain size and shape, the fraction of domain phase, and the location of each acceptor within the domain in an exceedingly complex manner, which has so far prevented exact rationalization in a closed formed analytical solution. Similar considerations can be raised about donors located inside the domains. Therefore, it is unsurprising that efforts to derive analytical solutions have either involved severe simplifying approximations or relied to some extent to numerical results, as described below.

The first model addressing this question was published by Gutierrez-Merino (1981), who derived expressions for the average rate of energy transfer, $\langle k_T \rangle$. Phase separation in binary phospholipid mixtures (with one component partially labelled with donor and the other component with acceptor, considering a triangular lattice for the lipids in the gel phase) was studied. It was possible to distinguish between gel-phase domains formed from the bulk fluid and the formation of fluid domains from the bulk gel. The model ingeniously establishes the relationship between
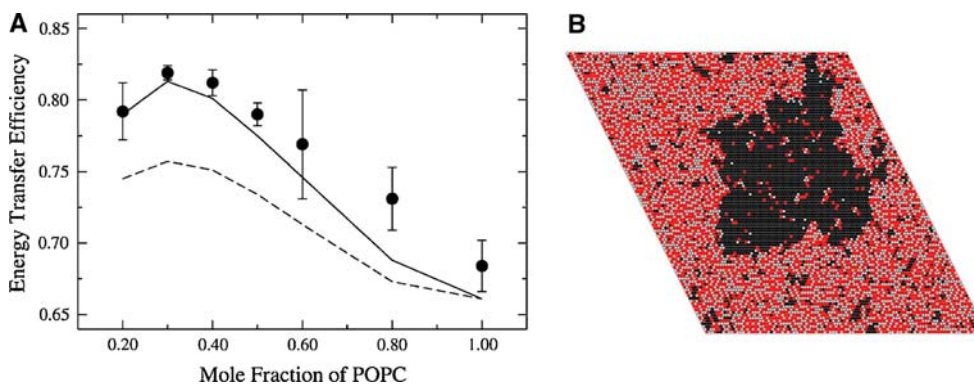
Fig. 5 **a** Dependence of FRET efficiency on POPC mole fraction in LUVs of BSM/Chol/POPC. FRET experiments (*solid circles*) were performed on vesicles with equimolar mixtures of BSM and Chol and varying POPC content (*abscissa axis*). The Marina Blue-POPE (D) and NBD-POPE (**a**) concentrations are kept at 0.5 and 0.75 mol%, respectively, of the total lipid. The *solid line* represents the Monte Carlo simulation results calculated for the same lipid compositions and probe concentrations, using unlike nearest-neighbour interaction terms $\omega_{SC} = -350$, $\omega_{SP} = 300$, and $\omega_{CP} = 200$ cal/mol. The *dashed*

line corresponds to a calculation where ω_{SP} was changed to 250 cal/mol. **b** Snapshot of one monolayer of an equilibrated Monte Carlo simulation of SM/Chol/POPC 35:35:30. POPC molecules are represented by the *black lattice sites*, Chol molecules are represented by the *red sites*, and SM molecules are represented by the *white sites*. The lattice size was 100×100 (10,000 lipids) and the lipid–lipid interaction terms were $\omega_{SC} = -350$, $\omega_{SP} = 300$, and $\omega_{CP} = 200$ cal/mol. Reprinted from Frazier et al. (2007) with permission. Copyright 2007 Biophysical Society

$\langle k_T \rangle$ and the size of the domains (whose shape is considered the most compact, i.e., round or hexagonal). However, there are some limitations to the model, namely, the simplification that underlies the formalism, which consists of considering FRET only to the nearest neighbours in the gel-phase lattice (if labelled with acceptor) or from the two external circular layers of the fluid-phase domains. On the other hand, because the experimental observable is the average FRET efficiency given by:

$$\langle E \rangle = \left\langle \frac{k_T}{k_T + k_D} \right\rangle \quad (17)$$

where k_D is the donor intrinsic decay rate coefficient, the relationship with $\langle k_T \rangle$ is not straightforward. It is proposed that if the setting of experimental conditions is such that $\langle E \rangle$ is low (namely, $\langle k_T \rangle \ll \langle k_D \rangle$), then $\langle E \rangle \cong \langle k_T \rangle / \langle k_D \rangle$. However, low-accuracy FRET efficiencies are difficult to measure experimentally.

Towles et al. (2007) published two different analytical approaches recently. In the first, the contribution to the donor decay of acceptors populating a shell of thickness δ at any distance (projected in the bilayer plane) $R - \delta/2 < R < R + \delta/2$ from the donor is computed, by dividing the FRET contribution due to acceptors situated beyond the shell's inner radius by that due to acceptors situated beyond the outer radius:

$$i_{DA}(t)_{\text{shell}} = i_D(t) \frac{[\rho_{cis}(t)\rho_{trans}(t)]_{R_e = R - \delta/2}}{[\rho_{cis}(t)\rho_{trans}(t)]_{R_e = R + \delta/2}} \quad (18)$$

From the contribution of each infinitely narrow shell, the overall donor decay is computed:

$$i_{DA}(t) = i_D(t) \prod_{i=1}^{\infty} \frac{[\rho_{cis}(t)\rho_{trans}(t)]_{R_e = \delta i}}{[\rho_{cis}(t)\rho_{trans}(t)]_{R_e = \delta(i+1)}} \quad (19)$$

Because of the acceptor distribution heterogeneity, the average acceptor concentration c (needed to calculate the ρ functions on the right hand side of the preceding equation) varies from shell to shell, and is an average of the concentrations in the two phases, weighted by the area fraction of each phase inside the shell under consideration. Variation of the fractional areas with distance to a given donor is not trivial. For the two cases of donors inside and outside the domains, the weights are calculated making use of ensemble-averaged radial distribution functions (RDFs), which are related to the probability of finding a circular monodisperse domain at a distance R from the donor. These RDFs are computed numerically. For each value of overall fractional area of each phase, a universal curve is obtained if a reduced distance (R divided by the domain size) is used as independent variable. Therefore, the model is not entirely analytical, as it ultimately depends on numerical calculations. The authors publish analytical fitting functions to their RDFs for specific values of the area fraction of the domain phase.

The subtle approximation in this model resides in the fact that instead of averaging over the decay kinetics of the donor ensemble (composed of an impossibly large number of non-equivalent donors, differing both in whether they are inside or outside the domains and, more crucially, in their location relative to the underlying domain structure, which determines the survival probability of each), all donors are treated as equivalent (except only for their being either inside or

outside a domain), sensing a distance-dependent ensemble average acceptor density which is calculated from the above mentioned radial distribution functions. That is, averaging is performed at the level of sensed acceptor density rather than at the level of survival rates of individual donors, which is reminiscent of the so-called "mean concentration model" (Liu et al. 1993, 2000a; Loura and Prieto 2000). The advantage of this necessarily complex and still approximate (but satisfactorily tested by analysis of numerically simulated decays) model is that it yields the domain size as a fitting parameter. Indeed, if R_0, the overall c value, K_{pD}, K_{pA}, the fraction and area per lipid of each phase, and all donor lifetime components, are known (in practice, some of these may be calculated from independent measurements, whereas others may be constrained using global analysis), the decay at a given time is a (very complex, but this is certainly unavoidable) implicit function of the domain size. In a separate paper (Towles and Dan 2007), the applicability of the formalism to polydisperse domains under different domain ordering regimes (hexagonal packing, totally random non-overlapping) was tested by comparison with numerical simulations (see preceding section). It was concluded that the method was especially suited to probing the size of domains up to $4R_0$, irrespective of domain polydispersity and packing, and confidence estimates are given as function of the recovered domain size/R_0 ratio.

Later the same year the authors proposed a different model, with three assumptions:

1. donors are distributed randomly within the (Chol-rich) domain;
2. the domains are disk-like; and
3. the domains are correlated across the bilayer leaflets (Brown et al. 2007a).

The FRET efficiency was calculated from the following expressions (Fung and Stryer 1978):

$$E = 1 - \frac{1}{\tau_0} \int_0^\infty \exp(-t/\tau_0)\exp[-n(S_1(t) + S_2(t))]\mathrm{d}t \quad (20)$$

where

$$S_1(t) = \int_{LL1}^\infty \left\{1 - \exp\left[-(t/\tau_0)(R_0/R)^6\right]\right\}2\pi r\mathrm{d}r \quad (21)$$

refers to FRET within the same bilayer leaflet (*cis*), whereas:

$$S_2(t) = \int_{LL2}^\infty \left\{1 - \exp\left[-(t/\tau_0)(R_0/R)^6\right]\right\}2\pi r\mathrm{d}r \quad (22)$$

reflects FRET between donors and acceptors in opposing leaflets (*trans*). The lower limits LL1 and LL2 in Eqs. 21

and 22 account for this difference. In the presence of domains, probes are either located in the same phase or in opposite phases. When both donor and acceptor are located in the same phase, LL1 is given by the sum of the molecular radii and LL2 is given by the bilayer thickness. If donor and acceptor are in different phases, then LL1 and LL2 become functions of domain radius. For the sake of averaging over the possible donor positions inside a circular domain, the authors take LL1 (closest approach distance between the donor in the domain and acceptor outside the domain) equal to 1/3 of the domain radius (because, for uniform distribution, the most probable distance to the centre is 2/3 of the radius). LL2 is estimated from this LL1 value by trivial geometric reasoning.

There are several limitations to this otherwise interesting model. First, it considers only two situations, donor and acceptor in the same (continuous) phase and in distinct (donor in the domains, acceptor outside the domains) phases. Therefore, the model does not consider the possibility of acceptors being located in domains (the effect of this can be reduced by selecting an acceptor with no preference for the domains). A most important issue regarding this model is that it is solely valid in the limit of infinite domain dilution. Otherwise, even disregarding the possibility of acceptors being located inside domains, the distribution function for donor–acceptor distance will no longer be uniform, as there will be excluded areas. This is not accounted for in the model, because it assumes uniform distribution of acceptors, apart from the exclusion distances LL1 and LL2. The authors acknowledge this to some extent, by stating that the model is not valid for the high lo (the domain phase in their assumption) phase fraction, before inaccurately claiming that such compositions are "not common biologically". Finally, whereas Eqs. 20–22 are used to calculate the FRET efficiency related to donors in the individual ld (E_{same}) or lo (E_{diff}) phases, these values are combined to produce the overall efficiency as an average:

$$E_{overall} = d_d E_{same} + d_o E_{diff} \quad (23)$$

weighed by the fraction of donors in the ld (d_d) and lo (d_o) phases. This equation, however, is incorrect, because it can be readily shown that the true weights are the fractions of fluorescence light emitted by each of the subpopulations, not the molecular fractions. The effects of these limitations are hard to estimate, because no numerical simulation results were presented to test the formalism.

Whereas, as far as we are aware, the Gutiérrez-Merino model has not been used to study lipid phase separation, and the first model by Towles et al. (2007) was only tested against simulated data, the latter model by these authors was applied to both the binary DMPC/Chol (Brown et al. 2007a) and ternary DOPC/DPPC/Chol (Brown et al.

2007b) mixtures. Regarding the binary system, steady-state FRET between donor DHE and acceptor 2-[12-[(5-dimethylamino-1-naphthalenesulfonyl)amino]dodecanoyl]-PC (dansyl-PC) was used to demonstrate domain formation. Whereas the lo/ld partition coefficient of DHE was assumed to be equal to that of Chol (readily available from the phase diagram), the acceptor was assumed to have complete preference for the disordered phase (as required in the authors' model), from the variation of dansyl-PC emission maximum as a function of Chol content. No domain sizes, however, were inferred for this mixture. Concerning the ternary system, the described formalism (modified to allow the introduction of polydispersity in domain size) was used with the same FRET pair. Contrary to the study of Buboltz et al. (2007b), the authors propose an extension of the two-phase region of this mixture (to include, e.g., the mole composition DOPC/DPPC/Chol 2:1:2). This opposite behaviour is possibly because of the enhanced sensitivity of this method for small domains (whereas the phase boundaries of Buboltz et al. (2007b) are obtained only in the infinite phase limit), but the application of the formalism to data points closer to the lo boundary (the authors attempt with as much as 0.7–0.8 of lo mole fraction) is, as commented above, incorrect. Therefore, and taking into consideration all the other simplifications in these authors' model, the size determinations (mapped over the phase diagram) must be viewed with caution. The authors also studied the POPC/DPPC/Chol system, where no extensive phase separation is detected, not even for the POPC/Chol 4:1 mixture. In fact, whereas this latter composition lies just inside the phase coexistence of the POPC/Chol binary system (de Almeida et al. 2003), the domains therein are expected to be too small for even FRET to detect (de Almeida et al. 2005).

Conclusions

In this review, the application of FRET methodology to the detection and characterization of membrane heterogeneity (membrane domains) at increasing complexity was described. It is not difficult to conclude that domains are absent, because in this case donor and acceptor should be randomly distributed throughout the membrane surface, and analytical solutions for the transfer kinetics are easily available. If phase separation exists, it is possible to perform detailed system modelling, and, because the range of FRET interaction is the same as the relevant domains in membranes (nanodomains), FRET is especially suited as a tool for their study. Also if the system topology is too complex, hampering the derivation of quantitative formalisms, it is possible to carry out numerical simulations of FRET, for comparison with the experimental data.

Time-resolved data are crucial for a detailed analysis, because the information lost on integration over time (i.e. steady-state) can be the ruling factor in discriminating among different models (i.e., topologies), which otherwise can lead to fluorescence intensity similar to that obtained from steady-state data. Additionally, time-resolved decays are free from inner-filter effects. On the other hand, scattering, always present in membrane suspensions, is much less important in time-resolved studies, because it can be dealt with in the deconvolution analysis. Also the fluorescence decay has an impressive dynamic range and signal/noise ratio, making it adequate to fit complex kinetic models. It was also shown in this review that a FRET experiment should be carefully designed, and, in addition to a favourable Förster radius, detailed photophysical characterization of the probes and determination of their phase preference (partition constant), should also be carried out in advance. This review, in addition to the relevant literature, also details the successive methodological steps that should be carried out.

The lo/ld phase co-existence is the most relevant in biology, and it is directly connected to the raft concept. This type of phase is sometimes difficult to address via other techniques for example calorimetry, and FRET has been shown to be a successful approach. On the other hand, gel phases can sometimes prevent the incorporation of probes, and in FRET studies this situation is easily parameterized.

Quantitative FRET applications in microscopy will certainly increase in the next few years. Imaging techniques have been extensively used in the attempt to characterize lateral membrane heterogeneities both in model systems and in cellular models. Several studies have applied FRET microscopy methods, with success, to the problem of identifying membrane microdomains below the resolution limit of confocal microscopes (Rao and Mayor 2005). Use of fluorescent proteins as FRET donor and acceptor fusion tags has proved of great value, because it enables non-invasive characterization of the lateral distribution of membrane proteins in living cells, where dynamic processes affecting the distribution of membrane components could be potentially studied in real time. Because of the susceptibility of some fluorescent proteins to homo-FRET, it is also possible to perform quantitative FRET studies on the partition of membrane proteins to nanodomains using only one protein chimera (Varma and Mayor 1998; Sharma et al. 2004; Scolari et al. 2009). In the near future, it is expected that improvements in multi-wavelength and polarization-resolved imaging will lead to more widespread use of FRET imaging in studies of functional assemblies in cell membranes, and higher frame rates should be attainable (Owen et al. 2007).

References

Adair BD, Engelman DM (1994) Glycophorin A helical transmembrane domains dimerize in phospholipid bilayers: a resonance energy transfer study. Biochemistry 33:5539–5544

Almeida PFF, Vaz WLC, Thompson TE (1992) Lateral diffusion in the liquid-phases of dimyristoylphosphatidylcholine cholesterol lipid bilayers—a free-volume analysis. Biochemistry 31:6739–6747

Baumgart T, Hunt G, Farkas ER, Webb WW, Feigenson GW (2007) Fluorescence probe partitioning between lo/ld phases in lipid membranes. Biochim Biophys Acta 1768:2182–2194

Berney C, Danuser G (2003) FRET or no FRET: a quantitative comparison. Biophys J 84:3992–4010

Brown RE (1998) Sphingolipid organization in biomembranes: what physical studies of model membranes reveal. J Cell Sci 111:1–9

Brown AC, Towles KB, Wrenn SP (2007a) Measuring raft size as a function of membrane composition in PC-based systems: part I—binary systems. Langmuir 23:11180–11187

Brown AC, Towles KB, Wrenn SP (2007b) Measuring raft size as a function of membrane composition in PC-based systems: part II—ternary systems. Langmuir 23:11188–11196

Buboltz JT (2007) Steady-state probe-partitioning FRET: a simple and robust tool for the study of membrane phase behavior. Phys Rev E 76:021903

Buboltz JT, Bwalya C, Reyes S, Kamburov D (2007a) Stern–Volmer modeling of steady-state Förster energy transfer between dilute, freely diffusing membrane-bound fluorophores. J Chem Phys 127:215101

Buboltz JT, Bwalya C, Williams K, Schutzer M (2007b) High-resolution mapping of phase behavior in a ternary lipid mixture: do lipid-raft phase boundaries depend on the sample preparation procedure? Langmuir 23:11968–11971

Corry B, Jayatilaka D, Rigby P (2005) A flexible approach to the calculation of resonance energy transfer efficiency between multiple donors and acceptors in complex geometries. Biophys J 89:3822–3836

Coutinho A, Loura LM, Fedorov A, Prieto M (2008) Pinched multilamellar structure of aggregates of lysozyme and phosphatidylserine-containing membranes revealed by FRET. Biophys J 95:4726–4736

Davenport L (1997) Fluorescence probes for studying membrane heterogeneity. Meth Enzymol 278:487–512

Davenport L, Dale RE, Bisby RH, Cundall RB (1985) Transverse location of the fluorescent probe 1,6-diphenyl-1,3,5-hexatriene in model lipid bilayer membrane systems by resonance energy transfer. Biochemistry 24:4097–4108

de Almeida RFM, Loura LMS, Fedorov A, Prieto M (2002) Nonequilibrium phenomena in the phase separation of a two-component lipid bilayer. Biophys J 82:823–834

de Almeida RFM, Fedorov A, Prieto M (2003) Sphingomyelin/phosphatidylcholine/cholesterol phase diagram: boundaries and composition of lipid rafts. Biophys J 85:2406–2416

de Almeida RFM, Loura LMS, Prieto M, Watts A, Fedorov A, Barrantes FJ (2004) Cholesterol modulates the organization of the γM4 transmembrane domain of the muscle nicotinic acetylcholine receptor. Biophys J 86:2261–2272

de Almeida RFM, Loura LMS, Fedorov A, Prieto M (2005) Lipid rafts have different sizes depending on membrane composition: a time-resolved fluorescence resonance energy transfer study. J Mol Biol 346:1109–1120

de Almeida RFM, Borst J, Fedorov A, Prieto M, Visser AJWG (2007) Complexity of lipid domains and rafts in giant unilamellar vesicles revealed by combining imaging and microscopic and macroscopic time-resolved fluorescence. Biophys J 93:539–553

Demidov AA (1999) Use of a Monte Carlo method in the problem of energy migration in molecular complexes. In: Andrews DL, Demidov AA (eds) Resonance energy transfer. Wiley, New York., pp 435–465

Dietrich C, Bagatolli LA, Volovyk ZN, Thompson NL, Levi Jacobson K, Gratton E (2001) Lipid rafts reconstituted in model membranes. Biophys J 80:1417–1428

Fernandes F, Loura LMS, Prieto M, Koehorst R, Spruijt R, Hemminga MA (2003) Dependence of M13 major coat protein oligomerization and lateral segregation on bilayer composition. Biophys J 85:2430–2441

Fernandes F, Loura LMS, Fedorov A, Prieto M (2006) Absence of clustering of phosphatidylinositol-(4,5)-bisphosphate in fluid phosphatidylcholine. J Lipid Res 47:1521–1525

Fernandes F, Loura LMS, Chichón FJ, Carrascosa JL, Fedorov A, Prieto M (2008) Role of helix 0 of the N-BAR domain in membrane curvature generation. Biophys J 94:3065–3073

Förster T (1949) Experimentelle und theoretische Untersuchung des Zwischenmolekularen übergangs von Elektrinenanregungsenergie. Z Naturforsch 4a:321–327

Franquelim HG, Loura LM, Santos NC, Castanho MA (2008) Sifuvirtide screens rigid membrane surfaces. Establishment of a correlation between efficacy and membrane domain selectivity among HIV fusion inhibitor peptides. J Am Chem Soc 130:6215–6223

Frazier ML, Wright JR, Pokorny A, Almeida PF (2007) Investigation of domain formation in sphingomyelin/cholesterol/POPC mixtures by fluorescence resonance energy transfer and Monte Carlo simulations. Biophys J 92:2422–2433

Frederix P, de Beer EL, Hamelink W, Gerritsen HC (2002) Dynamic Monte Carlo simulations to model FRET and photobleaching in systems with multiple donor–acceptor interactions. J. Phys Chem B 106:6793–6801

Fung BK, Stryer L (1978) Surface density determination in membranes by fluorescence energy transfer. Biochemistry 17:5241–5248

Goñi FM, Alonso A, Bagatolli LA, Brown RE, Marsh D, Prieto M, Thewalt JL (2008) Phase diagrams of lipid mixtures relevant to the study of membrane rafts. Biochim Biophys Acta 1781:665–684

Goswami D, Gowrishankar K, Bilgrami S, Ghosh S, Raghupathy R, Chadda R, Vishwakarma R, Rao M, Mayor S (2008) Nanoclusters of GPI-anchored proteins are formed by cortical actin-driven activity. Cell 135:1085–1097

Gutierrez-Merino C (1981) Quantitation of the Förster energy transfer for two-dimensional systems. I. Lateral phase separation in unilamellar vesicles formed by binary phospholipid mixtures. Biophys Chem 14:247–257

Hell SW (2009) Microscopy and its focal switch. Nat Methods 6:24–32

Holt A, de Almeida RFM, Nyholm TK, Loura LMS, Daily AE, Staffhorst RW, Rijkers DT, Koeppe RE 2nd, Prieto M, Killian JA (2008) Is there a preferential interaction between cholesterol and tryptophan residues in membrane proteins? Biochemistry 47:2638–2649

Ipsen JH, Karlström G, Mouritsen OG, Wennerström H, Zuckermann MJ (1987) Phase equilibria in the phosphatidylcholine–cholesterol system. Biochim Biophys Acta 905:162–172

Jacobson K, Mouritsen OG, Anderson RG (2007) Lipid rafts: at a crossroad between cell biology and physics. Nat Cell Biol 9:7–14

Jørgensen K, Mouritsen OG (1995) Phase separation dynamics and lateral organization of two-component lipid membranes. Biophys J 69:942–954

Kiskowski MA, Kenworthy AK (2007) In silico characterization of resonance energy transfer for disk-shaped membrane domains. Biophys J 92:3040–3051

Leidy C, Wolkers WF, Jørgensen K, Mouritsen OG, Crowe JH (2001) Lateral organization and domain formation in a two-component lipid membrane system. Biophys J 80:1819–1828

Li M, Reddy LG, Bennett R, Silva ND Jr, Jones LR, Thomas DD (1999) A fluorescence energy transfer method for analysing protein oligomeric structure: application to phospholamban. Biophys J 76:2587–2599

Liu YS, Li L, Ni S, Winnik M (1993) Recovery of acceptor concentration distribution in direct energy transfer experiments. Chem Phys 177:579–589

London E (2005) How principles of domain formation in model membranes may explain ambiguities concerning lipid raft formation in cells. Biochim Biophys Acta 1746:203–220

Loura LMS, Prieto M (2000) Resonance energy transfer in heterogeneous planar and bilayer systems: theory and simulation. J Phys Chem B 104:6911–6919

Loura LMS, Fedorov A, Prieto M (1996) Resonance energy transfer in a model system of membranes: application to gel and liquid crystalline phases. Biophys J 71:1823–1836

Loura LMS, Fedorov A, Prieto M (2000a) Membrane probe distribution heterogeneity: a resonance energy transfer study. J Phys Chem B 104:6920–6931

Loura LMS, Fedorov A, Prieto M (2000b) Partition of membrane probes in a gel/fluid two-component lipid system: a fluorescence resonance energy transfer study. Biochim Biophys Acta 1467:101–112

Loura LMS, Fedorov A, Prieto M (2001a) Exclusion of a cholesterol analog from the cholesterol-rich phase in model membranes. Biochim Biophys Acta 1511:236–243

Loura LMS, Fedorov A, Prieto M (2001b) Fluid–fluid membrane microheterogeneity: a fluorescence resonance energy transfer study. Biophys J 80:776–788

Loura LMS, Coutinho A, Silva A, Fedorov A, Prieto M (2006) Structural effects of a basic peptide on the organization of dipalmitoylphosphatidylcholine/dipalmitoylphosphatidylserine membranes: a fluorescent resonance energy transfer study. J Phys Chem B 110:8130–8141

Mateo CR, Acuna AU, Brochon J-C (1995) Liquid-crystalline phases of cholesterol lipid bilayers as revealed by the fluorescence of trans-parinaric acid. Biophys J 68:978–987

Mesquita MMRS, Melo E, Thompson TE, Vaz WLC (2000) Partitioning of amphiphiles between coexisting ordered and disordered phases in two-phase lipid bilayer membranes. Biophys J 78:3019–3025

Morrow MR, Davis JH, Sharom FJ, Lamb MP (1986) Studies on the interaction of human erythrocyte band 3 with membrane lipids using deuterium nuclear magnetic resonance and differential scanning calorimetry. Biochim Biophys Acta 858:13–20

Mouritsen OG (2005) Life—as a matter of fat. The emerging science of lipidomics. Springer, Heidelberg

Mouritsen OG, Bloom M (1984) Mattress model of lipid–protein interactions in membranes. Biophys J 46:141–153

Niemelä PS, Hyvönen MT, Vattulainen I (2009) Atom-scale molecular interactions in lipid raft mixtures. Biochim Biophys Acta 1788:122–135

Owen DM, Neil MA, French PM, Magee AI (2007) Optical techniques for imaging membrane lipid microdomains in living cells. Semin Cell Dev Biol 18:591–598

Pandit SA, Jakobsson E, Scott HL (2004) Simulation of the early stages of nano-domain formation in mixed bilayers of sphingomyelin, cholesterol, and dioleylphosphatidylcholine. Biophys J 87:3312–3322

Pedersen S, Jørgensen K, Bækmark TR, Mouritsen OG (1996) Indirect evidence for lipid–domain formation in the transition region of phospholipid bilayers by two-probe fluorescence energy transfer. Biophys J 71:554–560

Pokorny A, Yandek LE, Elegbede AI, Hinderliter A, Almeida PFF (2006) Temperature and composition dependence of the interaction of δ-lysin with ternary mixtures of sphingomyelin/cholesterol/POPC. Biophys J 91:2184–2197

Putzel GG, Schick M (2008) Phenomenological model and phase behavior of saturated and unsaturated lipids and cholesterol. Biophys J 95:4756–4762

Rao M, Mayor S (2005) Use of Forster's resonance energy transfer microscopy to study lipid rafts. Biochim Biophys Acta 1746:221–233

Redfern DA, Gericke A (2004) Domain formation in phosphatidylinositol monophosphate/phosphatidylcholine mixed vesicles. Biophys J 86:2980–2992

Redfern DA, Gericke A (2005) pH-dependent domain formation in phosphatidylinositol polyphosphate/phosphatidylcholine mixed vesicles. J Lipid Res 46:504–515

Ries J, Chiantia S, Schwille P (2009) Accurate determination of membrane dynamics with line-scan FCS. Biophys J 96:1999–2008

Santos NC, Prieto M, Castanho M (2003) Quantifying molecular partition into model systems of biomembranes. An emphasis on optical spectroscopic methods. Biochim Biophys Acta 1612:123–135

Scolari S, Engel S, Krebs N, Plazzo AP, De Almeida RF, Prieto M, Veit M, Herrmann A (2009) Lateral distribution of the transmembrane domain of influenza virus hemagglutinin revealed by time-resolved fluorescence imaging. J Biol Chem 284:15708–15716

Sergé A, Bertaux N, Rigneault H, Marguet D (2008) Dynamic multiple-target tracing to probe spatiotemporal cartography of cell membranes. Nat Methods 5:671–672

Sharma P, Varma R, Sarasij RC, Ira, Gousset K, Krishnamoorthy G, Rao M, Mayor S (2004) Nanoscale organization of multiple GPI-anchored proteins in living cell membranes. Cell 116:577–589

Shimshick EJ, McConnel HM (1973) Lateral phase separation in phospholipid membranes. Biochemistry 12:2351–2360

Silva LC, de Almeida RFM, Castro BM, Fedorov A, Prieto M (2007) Ceramide-domain formation and collapse in lipid rafts: membrane reorganization by an apoptotic lipid. Biophys J 92:502–516

Silvius JR (2003) Fluorescence energy transfer reveals microdomain formation at physiological temperatures in lipid mixtures modeling the outer leaflet of the plasma membrane. Biophys J 85:1034–1045

Simons K, Vaz WL (2004) Model systems, lipid rafts, and cell membranes. Annu Rev Biophys Biomol Struct 33:269–295

Singer SJ, Nicholson GL (1972) The fluid mosaic model of the structure of cell membranes. Science 175:720–731

Smaby JM, Momsen MM, Brockman HL, Brown RE (1997) Phosphatidylcholine acyl unsaturation modulates the decrease in interfacial elasticity induced by cholesterol. Biophys J 73:1492–1505

Snyder B, Freire E (1982) Fluorescence energy transfer in two dimensions. A numeric solution for random and non-random distributions. Biophys J 40:137–148

Stilwell W, Jenski LJ, Zerouga M, Dumaual AC (2000) Detection of lipid domains in docosahexaenoic acid-rich bilayers by acyl chain-specific FRET probes. Chem Phys Lipids 104:113–132

Stryer L, Haugland RP (1967) Energy transfer: a spectroscopic ruler. Proc Natl Acad Sci USA 58:719–726

Takanishi CL, Bykova EA, Cheng W, Zheng J (2006) GFP-based FRET analysis in live cells. Brain Res 1091:132–139

Towles KB, Dan N (2007) Determination of membrane domain size by fluorescence resonance energy transfer: effects of domain polydispersity and packing. Langmuir 23:4737–4739

Towles KB, Brown AC, Wrenn SP, Dan N (2007) Effect of membrane microheterogeneity and domain size on fluorescence resonance energy transfer. Biophys J 93:655–667

Van Der Meer B, Coker V III, Chen S-YS (1994) Resonance energy transfer: theory and data. VCH Publishers, New York

Varma R, Mayor S (1998) GPI-anchored proteins are organized in submicron domains at the cell surface. Nature 394:798–801

Veatch SL, Keller SL (2002) Organization in lipid membranes containing cholesterol. Phys Rev Lett 89:268101

Veatch SL, Keller SL (2003) Separation of liquid phases in giant vesicles of ternary mixtures of phospholipids and cholesterol. Biophys J 85:3074–3083

Veatch SL, Keller SL (2005) Seeing spots: complex phase behavior in simple membranes. Biochim Biophys Acta 1746:172–185

Veatch SL, Polozov IV, Gawrisch K, Keller SL (2004) Liquid domains in vesicles investigated by NMR and fluorescence microscopy. Biophys J 86:2910–2922

Veatch SL, Keller SL, Gawrisch K (2007) Critical fluctuations in domain-forming lipid mixtures. Proc Natl Acad Sci USA 104:17650–17655

Veiga AS, Santos NC, Loura LMS, Fedorov A, Castanho MA (2004) HIV fusion inhibitor peptide T-1249 is able to insert or adsorb to lipidic bilayers. Putative correlation with improved efficiency. J Am Chem Soc 126:14758–14763

Wolber PK, Hudson BS (1979) An analytical solution to the Förster energy transfer problem in two dimensions. Biophys J 28:197–210